

SOLUTION OF THE INVERSE RADIATION PROBLEM FOR ANISOTROPICALLY SCATTERING MEDIUM USING THE CONTROL VOLUME FINITE ELEMENT METHOD

by

Hajer GRISSA*, **Faouzi ASKRI**, **Fethi ALBOUCHI**,
and Sassi BEN NASRRALLAH

Ecole Nationale d'Ingénieurs de Monastir, Laboratoire d'Etudes des Systèmes Thermiques et Energétiques (LESTE), Monastir, Tunisia

Original scientific paper
UDC: 536.25:517.96
DOI: 10.2298/TSCI1002373G

In this paper, an inverse analysis is performed for the estimation of radiative parameters from the measured temperature profile in an absorbing, emitting, and anisotropically scattering medium. The control volume finite element method is employed to solve the direct problem in a 3-D rectangular furnace. The inverse problem is formulated as an optimization problem between the calculated and the experimental data and the Levenberg-Marquardt method is used for its solution. The sensitivity analysis is made in order to determine whether it is possible to identify the parameters. Also, the effects of angular and spatial grid numbers and the initial guesses on the accuracy of the inverse problem are investigated. This method combination, which is applied for the first time to solve 3-D inverse radiation problem, has been found to accurately predict the unknown parameters.

Key words: *inverse radiation problem, control volume finite element method, Levenberg-Marquardt method, parameter estimation, furnace, 3-D*

Introduction

Radiative properties of particles constituting a semi transparent medium can be theoretically determined using the complex refractive index, the shape, size, and volume fraction distribution of the particles. In one hand, the shape of the particles is usually irregular and random; therefore, it is necessary to assume an average, smooth shape, such as a sphere, to determine particle properties theoretically. In the other hand, the complex index of refraction is a function of the wavelength of the incident radiation and physical and chemical properties of the material. For these reasons, it is preferable to determine the relevant radiative properties from experiments. This can be accomplished by combining optical diagnostic techniques with inverse analyses of the radiative transfer problem [1].

The determination of medium properties such as absorption coefficient, scattering coefficient, phase function, and optical depth as well as surface properties such as emissivity and boundary temperature has been achieved by inverse radiation analysis from measured intensi-

* Corresponding author; e-mail: grissahajer@yahoo.fr

ties or temperatures [2-7]. A review of the references for inverse radiation analysis in 1986-1991 is available in the literature [8].

Despite the relatively large interest expressed in inverse radiation problem of parameter estimation, most of the work has considered one, or two-dimensional systems, and in these problems only a limited number of the unknown radiation parameters are estimated simultaneously. In the present study, absorbing and scattering coefficients and wall emissivity are estimated simultaneously. In the direct problem, the control volume finite element method (CVFEM) is used to solve the radiative transfer equation (RTE) in a 3-D participating media. In the inverse problem, the Levenberg-Marquardt method (LMM) is used to minimize the objective function. The effects of angular and spatial meshes refinement, initial guesses and measurement errors on the accuracy of the inverse analysis are investigated.

Direct radiation problem

Governing equations

We consider an absorbing, emitting, scattering, and gray medium. In this case, the mathematical formulation of the direct problem is given by:

$$[I(s, \vec{\Omega})] = (k_a + k_d)I(s, \vec{\Omega}) + k_a I_b(s) + \frac{k_d}{4\pi} \int_{\Omega} I(s, \vec{\Omega}') P(\vec{\Omega}, \vec{\Omega}') d\Omega' \quad (1)$$

where $I(s, \vec{\Omega})$ is the radiative intensity at position s in the direction $\vec{\Omega}$, k_a and k_d are absorbing and scattering coefficients, respectively, $I_b(s)$ – the total blackbody radiative intensity at the temperature of the medium, and $P(\vec{\Omega}, \vec{\Omega}')$ – the scattering phase function from the incoming $\vec{\Omega}'$ direction to the outgoing direction $\vec{\Omega}$.

The surface bounding medium is assumed gray and emits and reflects diffusely. So, the radiation boundary condition can be written as:

$$I_w(\vec{\Omega}) = \frac{\varepsilon_w \sigma_{SB} T_w^4}{\pi} + \frac{1 - \varepsilon_w}{\pi} \int_{\Omega_w} I_w(\vec{\Omega}') |\vec{\Omega} \cdot \vec{n}_w| d\Omega' \quad \text{if } \vec{\Omega} \cdot \vec{n}_w > 0 \quad (2)$$

where ε_w is the wall emissivity and \vec{n}_w is the unit normal vector to the wall.

The temperature distribution is determined from the following energy equation with a volumetric heat source of q :

$$q = k_a 4\sigma_{SB} T^4(s) + \int_{\Omega} I(s, \vec{\Omega}) d\Omega \quad (3)$$

The direct problem of concern here is to find the temperature distribution $T(s)$ for known radiative parameters such as absorbing and scattering coefficients, wall emissivity and phase function.

Numerical resolution of the direct problem

The control volume finite element method has been demonstrated to be successful in the solution of radiative transfer in 3-D rectangular enclosures [9], as well as for the non-axisymmetric radiative problems [10], and also for the solution of radiative transfer problems in complex geometries [11]. In [9], Grissa *et al.* have studied four benchmark problems of radiative heat transfer and they found that the CVFEM is accurate and efficient.

In the CVFEM, the spatial and the angular domains are divided into a finite number of control volumes and control solid angles, respectively.

For angular discretization, the total solid angle is subdivided into $(N_\varphi \times N_\theta)$ control solid angles as depicted in fig. 1, where $\Delta\varphi = (\varphi^+ - \varphi^-) = 2\pi/N_\varphi$ and $\Delta\theta = (\theta^+ - \theta^-) = \pi/N_\theta$. N_φ and N_θ represent numbers of control angle in the azimuthal and polar angle directions, respectively. These $(N_\varphi \times N_\theta)$ control solid angles are non-overlapping and their sum is 4π .

The control solid angle $\Delta\Omega^{mn}$ is expressed by:

$$\Delta\Omega^{mn} = \int_{\varphi^-}^{\varphi^+} \int_{\theta^-}^{\theta^+} \sin\theta d\theta d\varphi \quad (4)$$

For spatial discretization, the domain (e_x, e_y) is subdivided into three-node triangular elements and control surfaces are created around each node N by joining the centroids of the elements to midpoints of the corresponding sides, fig. 2(a). Then, to create the control volume V_{ijk} , fig. 2(b), the control surface is multiplied by z for nodes within calculation domain (and by $z/2$ when nodes are in boundaries) where z is the step of calculation in e_z direction.

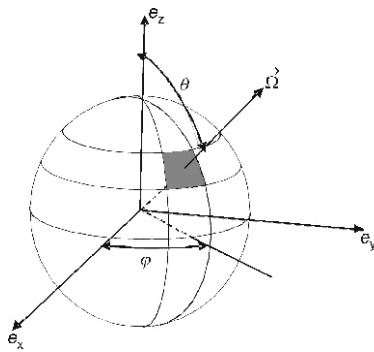


Figure 1. Angular discretization

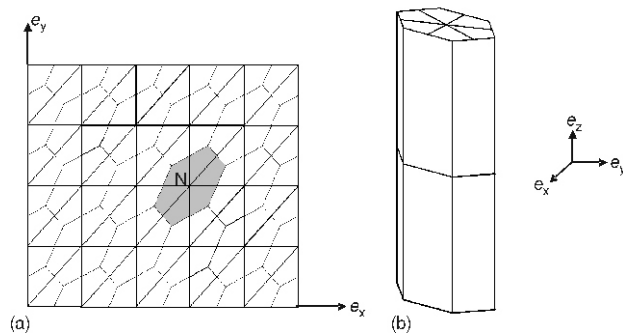


Figure 2. Spatial discretization

(a) discretization in (e_x, e_y) plane, (b) control volume V_{ijk}

In the first, the radiative transfer equation integrated over both control volume and control solid angle gives:

$$\Delta V_{ijk} \Delta\Omega^{mn} [I(s, \vec{\Omega}) - k_a I_b(s)] d\Omega dV = \Delta V_{ijk} \Delta\Omega^{mn} (k_a - k_d) I(s, \vec{\Omega}) d\Omega dV + \Delta V_{ijk} \Delta\Omega^{mn} \frac{k_d}{4\pi} \int_{\Omega} I(s, \vec{\Omega}') P(\vec{\Omega}, \vec{\Omega}') d\Omega' d\Omega dV \quad (5)$$

To approximate the integrals that represent the extinction, emission and in-scattering contributions, the radiation intensity is considered constant within V_{ijk} and Ω^{mn} and is evaluated at the centroid of the control volume and at the centre direction of the control solid angle. For the term on the left-hand side in eq. 5, the divergence theorem, the skew positive coefficient upwind (SPCU), and step schemes are used to calculate the corresponding quantity.

The final algebraic equation of the RTE is given by the following expression [9]:

$$\begin{aligned} & \gamma_{1ijk}^{mn} I_{ij}^{mn} - \gamma_{2ijk}^{mn} I_{i1jk}^{mn} - \gamma_{3ijk}^{mn} I_{i1j1k}^{mn} - \gamma_{41ijk}^{mn} I_{ij1k}^{mn} - \gamma_{5ijk}^{mn} I_{i1jk}^{mn} \\ & \gamma_{6ijk}^{mn} I_{i1j1k}^{mn} - \gamma_{7ijk}^{mn} I_{ijk}^{mn} - \gamma_{8ijk}^{mn} I_{ijk}^{mn} - \alpha_{ijk}^{mnmn} I_{ijk}^{mn} - \delta_{ijk}^{mn} \end{aligned} \quad (6)$$

Then, the algebraic eq. (6) is written in the following matrix form [9]

$$AI = b$$

The obtained matrix system is solved using the conditioned conjugate gradient squared method (CCGS). A detailed calculation can be found in ref. [9].

Equations (1) and (3) are coupled and must be solved iteratively to yield the radiation and the temperature fields. The computational procedure is as follows:

- Step 1: Assume the temperature distribution,
- Step 2: Calculate the total blackbody radiative intensity I_b using the given temperature distribution,
- Step 3: Solve the radiative transfer equation to obtain the radiative intensity I ,
- Step 4: Solve the energy equation (eq. 3) to update the temperature field, and
- Step 5: If the radiation and the temperature fields are not converged, go to Step 2.

Parameter identification procedure

The estimation of radiative parameters is achieved by a minimization of the objective function defined in eq. 8. This function is expressed by the square sum of errors between computed temperature obtained from direct problem, $T_i(\vec{\beta})$, and measured temperature, Y_i , at i measurement position:

$$J(\vec{\beta}) = \sum_{i=1}^l [Y_i - T_i(\vec{\beta})]^2 \quad (8)$$

where l is the total number of measurement points and $\vec{\beta}$ – the unknown parameters vector.

Sensitivity analysis

This study is essential before starting the parameter identification procedure; in fact it allows to determine if the parameters could be simultaneously estimated.

The sensitivity coefficients X_{ij} are defined as the first derivative of the estimated temperature at i measurement position, $T_i(\vec{\beta})$, with respect to the unknown parameter, β_j , that is:

$$X_{ij} = \frac{\partial T_i(\vec{\beta})}{\partial \beta_j}, \quad i = 1, \dots, l \quad \text{and} \quad j = 1, \dots, n_p \quad (9)$$

where n_p is the number of unknown parameters.

Physically, X_{ij} is a measure of the effects of changes in unknown parameters on estimated temperature. It is calculated from the finite difference approximation as:

$$X_{ij} = \frac{T_i(\beta_1, \dots, \beta_j + \delta\beta_j, \dots, \beta_{n_p}) - T_i(\beta_1, \dots, \beta_j, \dots, \beta_{n_p})}{\delta\beta_j} \quad (10)$$

where $\delta\beta_j = 10^{-4}\beta_j$.

For the comparison of the sensitivity coefficients and when the parameters do not have the same units, the following dimensionless quantities are used for the study of sensitivity:

$$\bar{X}_{ij} = \frac{T_i(\beta_1, \dots, \beta_j + \delta\beta_j, \dots, \beta_{n_p}) - T_i(\beta_1, \dots, \beta_j, \dots, \beta_{n_p})}{\delta\beta_j} \beta_j \quad (11)$$

The sensitivity analysis consists of studying the evolution of the different sensitivity coefficients vs. an explicative variable (position). In general, these coefficients must be large and uncorrelated with each other.

Parameter identification method

The minimization of the objective function is performed by the LMM which is used in several researches [1, 12-14].

The eq. 8 can be written as:

$$J = \bar{D}^T \bar{D} \quad (12)$$

where D_i is the difference between the measured and computed temperatures:

$$D_i = Y_i - T_i(\bar{\beta}) \quad (13)$$

Minimizing J with respect to $\bar{\beta}$ is equivalent to make its derivatives equal to zero:

$$\frac{\partial J}{\partial \bar{\beta}} = \frac{\partial(\bar{D}^T \bar{D})}{\partial \bar{\beta}} = 0 \quad (14)$$

In this equation, the vector \bar{D} is expanded in a Taylor series and only the first order terms are retained. To damp oscillations and instabilities due to the ill-conditioned character of the problem, a damping parameter, λ , is added to yield the LMM [15]. The iterative process is expressed as:

$$\bar{\beta}^{k+1} = \bar{\beta}^k + \Delta \bar{\beta}^k \quad (15)$$

where

$$\Delta \bar{\beta}^k = \frac{1}{(X^k)^T X^k + \lambda^k I} (X^k)^T \bar{D}^k \quad (16)$$

I and X denote the identity and the sensitivity matrix, respectively, and the superscript k denotes the iteration number.

The iterative procedure is continued until the convergence criterion:

$$\left| \bar{\beta}^{k+1} - \bar{\beta}^k \right| < 10^{-5} \quad (17)$$

is satisfied.

Computational algorithm

The steps of reconstructing radiative parameters are summarized as follows.

It is assumed that the temperature is measured, *i. e.* Y is given. We choose an initial set of parameters $\bar{\beta}^0$ and an initial value of the damping parameter $\lambda^0 = 0.001$.

The iteration number is initialized ($k = 0$). Then,

- Step 1: Solve the direct problem with the available estimate β^k in order to obtain the temperature vector $\bar{T}(\bar{\beta}^k)$; then compute the objective function J^k , as defined in eq. 8,
- Step 2: Compute the sensitivity matrix from eq. 10,
- Step 3: Calculate $\bar{\beta}^{k+1}$ by using eq. 15,
- Step 4: Compute $I(s, \bar{\Omega})$ in eq. 1 by solving the direct problem with boundary condition of eq. 2 and determine the distribution of temperature $\bar{T}(\bar{\beta}^{k+1})$ from the energy equation.
- Step 5: Calculate the objective function J^{k+1} ,
- Step 6: If $J^{k+1} > J^k$ then $\lambda^{k+1} = 10\lambda^k$, $J^{k+1} < J^k$ and return to step 2; otherwise, $\lambda^{k+1} = \lambda^k/10$ and the inverse procedure is continued, and
- Step 7: Check the stopping criterion (eq. 17). If it is satisfied then all calculation steps are terminated; else, replace $k+1$ by k and return to step 2.

Results

A 3-D furnace ($2 \text{ m} \times 2 \text{ m} \times 4 \text{ m}$) enclosing an absorbing, emitting and anisotropic scattering medium is considered. The exact value of both k_a and k_d is 0.5 m^{-1} . The walls are gray and with emissivity being 0.8. The temperatures of walls are all $T_w = 1000 \text{ K}$. A uniform volumetric heat source of $q = 5 \text{ kW/m}^3$ is prescribed in the medium.

An anisotropic scattering medium is considered with Delta Eddington phase function given by:

$$P(\vec{\Omega}, \vec{\Omega}') = 2f\delta(1 - \vec{\Omega} \cdot \vec{\Omega}') + (1-f)(1 + 3g\vec{\Omega} \cdot \vec{\Omega}') \quad (18)$$

where δ is the delta function and the values 0.781 and 0.868 are assigned to the constants f and g , respectively.

The direct radiation problem was solved by Fiveland [16] using the S_4 discrete ordinates solution by Coelho [17] using the hybrid finite volume/finite element discretization method and by Grissa *et al.* [9] using the CVFEM. However, to the knowledge of the authors, there is no work dealing specifically with the resolution of this inverse radiation problem.

In the inverse radiation problem, we assume that the temperature is known while the radiative properties, *i. e.* absorbing and scattering coefficients and phase function, and the boundary condition, *i. e.* emissivity of bottom wall ε_b , are regarded as unknown.

In order to obtain the measurement temperature, the direct problem is solved with the exact values of radiative parameters. Then, the obtained numerical solutions are considered as experimental data after adding small random noise:

$$Y = \bar{T}_{\text{exact}} + \xi\sigma \quad (19)$$

where σ is the standard deviation of the measurement errors and ξ – the Gaussian distributed random error within -2.576 to 2.576 for a 99% confidence bounds.

The CVFEM is used to predict the temperature distribution with $(N_x \times N_y \times N_z)$ spatial control volumes and $(N_\varphi \times N_\theta)$ control solid angles. N_x , N_y , and N_z represent numbers of control volumes in the e_x , e_y , and e_z directions, respectively.

The number of measurement points is set as $(N_z - 2)$ points evenly spaced in the centreline of medium, *i. e.*, $x = y = L/2$. All computations are realized with a Pentium (R)4 CPU 3.00 GHz.

For the sake of comparison, relative error E is defined as:

$$E_i[\%] = \frac{|\beta_{i \text{ estimated}} - \beta_{i \text{ exact}}|}{\beta_{i \text{ exact}}} \times 100 \quad (20)$$

Sensitivity coefficient analysis

The normalized sensitivity coefficients are calculated for the five parameters (k_a , k_d , ε_b , f , and g) using eq. (11). Results obtained are shown in fig. 3. One can note from fig. 3 that the model is very sensitive to the absorption and scattering coefficients and to the constant f of the phase function, whereas it is less sensitive to the bottom emissivity ε_b and to the constant g of the

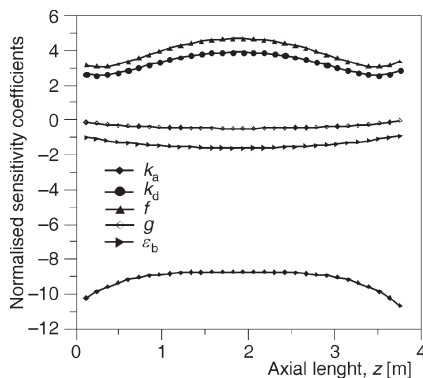


Figure 3. Spatial variations of normalized sensitivity coefficients of the radiative parameters

phase function. Moreover, the reduced sensitivity coefficients \bar{X}_{k_d} and \bar{X}_f are linearly dependents. So, it can not be identified simultaneously. Also, because of the low sensitivity of the constant g , this parameter can not be accurately estimated. Consequently, we assume that the phase function is known and we attempt to simultaneously estimate k_a , k_d , and ε_b .

Case 1. In this case, the initial values of k_a , k_d , and ε_b are set as 0.7 m, 0.3 m and 0.6, respectively. The standard deviation of measurement errors is equal to $\sigma = 0.07$ which corresponds to measured error of $\eta = 4.82\%$.

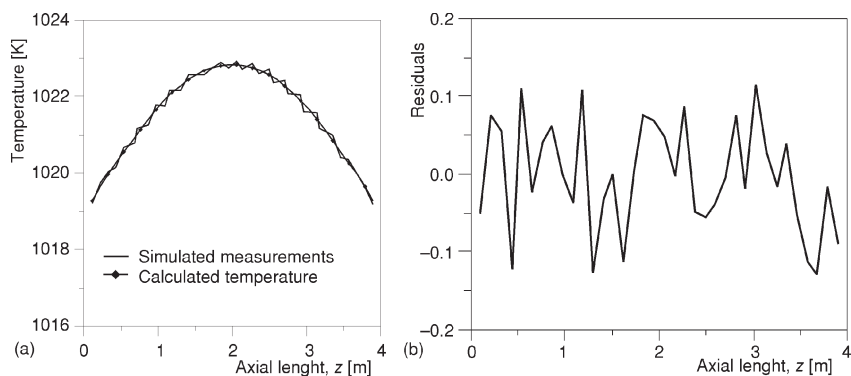
The effect of angular and spatial grid numbers on the precision of the estimation is examined by considering eight cases including different number of solid angles and control volumes. Table 1 shows the corresponding relative errors and CPU times. In one hand, the CPU time decreases by using a reduced number of angular or spatial meshes. On the other hand, it is observed that beyond $(10 \times 10 \times 20)$ control volumes and (8×4) solid angles, there is no significant change in the precision of the parameter estimation. Therefore, in the remainder of this work, we provide results considering $(10 \times 10 \times 20)$ control volumes and (8×4) solid angles.

Table 1. Relative error and CPU time using different angular and spatial discretizations

Number of control volumes	Number of solid angles	Inverse results			
		E [%]			CPU [s]
Effect of control volumes		k_a	k_d	ε_b	
$5 \times 5 \times 10$	8×4	0.24	0.38	1.62	230
$10 \times 10 \times 20$	8×4	0.21	0.321	0.88	387
$15 \times 15 \times 30$	8×4	0.208	0.32	0.879	566
$20 \times 20 \times 40$	8×4	0.208	0.319	0.878	733
Effect of solid angles					
$10 \times 10 \times 20$	6×4	0.228	0.34	0.9	291
$10 \times 10 \times 20$	8×4	0.21	0.321	0.88	387
$10 \times 10 \times 20$	12×6	0.208	0.32	0.878	524

We represent in fig. 4 the comparisons between the measured and the calculated temperatures using the estimated parameters and the residuals. We note a good agreement between curves. Besides, the residuals that represent the difference between the measured and the calculated temperature are random and centred on zero.

Figure 4.
(a) Measured and calculated temperature
(b) residuals



Case 2. In this case, we study the effect of noise level on the accuracy of the estimation through various standard deviations. It is observed, from tab. 2, that with the increase in the measurement errors from $\sigma = 0.0$ to $\sigma = 0.1$, the relative errors of parameters increase. For no measurement errors, the LMM requires more CPU time and the estimation is excellent with negligible errors.

Table 2. Effect of noise level on the accuracy of the estimation

	$\sigma = 0.0$ ($\eta = 0.0\%$)			$\sigma = 0.05$ ($\eta = 3.44\%$)			$\sigma = 0.1$ ($\eta = 6.88\%$)		
	Es.V.*	E [%]	CPU [s]	Es.V.*	E [%]	CPU [s]	Es.V.*	E [%]	CPU [s]
k_a [m^{-1}]	0.50001	$2 \cdot 10^{-3}$	757	0.50095	0.19	382	0.5031	0.62	396
k_d [m^{-1}]	0.49999	$2 \cdot 10^{-3}$		0.5015	0.30		0.4953	0.94	
ε_b	0.8009	0.11		0.8064	0.80		0.7783	2.71	

* Es.V. – estimated value

Case 3. The effect of the initial approximations on the accuracy of the inverse estimation is examined. At first, it is assumed that there are no measurement errors. The absorbing and scattering coefficients and the wall emissivity of the bottom surface are estimated simultaneously and the initial values of the parameters are taken arbitrary. Results from the LMM (tab. 3) show that excellent estimation can be obtained even with poor initial values.

Table 3. Effect of initial guesses on the accuracy of the estimation for no measurement errors

	Exact values	Initial values			Estimated values			Relative error [%]			Number of iterations		
		(a)	(b)	(c)	(a)	(b)	(c)	(a)	(b)	(c)	(a)	(b)	(c)
k_a [m^{-1}]	0.5	0.6	0.4	0.96	0.50001			$2 \cdot 10^{-3}$			9	9	10
k_d [m^{-1}]	0.5	0.3	0.7	0.48	0.49999			$2 \cdot 10^{-3}$					
ε_b	0.5	0.25	0.9	0.6	0.79907			0.116					

Let us examine the effect of initial guesses with measurement errors (the standard deviation of measurement errors is equal to $\sigma = 0.07$). Table 4 reveals that the relative errors are quite small even with measurement errors.

Table 4. Effect of initial guesses on the accuracy of the estimation with measurement errors

	Exact values	Initial values			Estimated values			Relative error [%]			Number of iterations		
		(a)	(b)	(c)	(a)	(b)	(c)	(a)	(b)	(c)	(a)	(b)	(c)
k_a [m^{-1}]	0.5	0.6	0.4	0.96	0.499			0.2			7	6	6
k_d [m^{-1}]	0.5	0.3	0.7	0.48	0.5016			0.32					
ε_b	0.5	0.25	0.9	0.6	0.79296			0.88					

Conclusions

An inverse radiation problem is solved for the simultaneous estimation of absorbing and scattering coefficients and wall emissivity in a 3-D furnace from the knowledge of temperature profile. The parameters' estimation possibility is analysed from a sensibility study. The optimization is achieved using the LMM. Several test cases involving different number of angular and spatial discretizations, measurement errors, and initial guesses are considered. The results show that beyond $(10 \times 10 \times 20)$ control volumes and (8×4) solid angles, there is no significant change in the precision of parameter estimation. Also, it is observed that the LMM does not require an accurate initial guesses of the unknown quantities even with noise measurement.

Nomenclature

\vec{D}	– vector which represent the difference between the measured and computed temperatures
\vec{D}_i	– i element of the vector D
E	– relative error
f	– constant of phase function, (0.781)
g	– constant of phase function, (0.868)
I	– radiative intensity, [$\text{Wm}^{-2}\text{sr}^{-1}$]
I	– identity matrix
J	– objective function
k_a	– absorbing coefficient, [m^{-1}]
k_d	– scattering coefficient, [m^{-1}]
L	– side length, [m]
l	– number of measurement points
\vec{n}	– unit normal vector
n_p	– number of unknown parameters
P	– scattering phase function
q	– volumetric heat source, [Wm^{-3}]
s	– position, [m]
T	– calculated temperature, [K]
T_{exact}	– calculated temperature with the exact values of the radiative parameters, [K]
X	– sensitivity matrix
Y	– measured temperature, [K]
x, y, z	– Cartesian co-ordinates

ΔV – control volume, [m^3]

Greek letters

$\vec{\beta}$	– unknown parameters vector
ε	– emissivity of a surface
η	– measured error, [%]
θ	– polar angle, [rad]
λ	– damping parameter
σ	– standard deviation of the measurement noise
σ_{SB}	– Stefan-Boltzman constant, [$\text{Wm}^{-2}\text{K}^{-4}$]
φ	– azimuthal angle, [rad]
Ω	– direction of propagation, [sr]
$\Delta\Omega$	– control angle, [sr]

Subscripts

b	– blackbody
w	– wall index

Superscripts

m, n, m', n'	– indices for directions
k	– iteration number
-	– reduced

References

- [1] Subramaniam, S., Menguc, M. P., Solution of the Inverse Radiation Problem for Inhomogeneous and Anisotropically Scattering Media Using Monte Carlo Technique, *Int. J. Heat Mass Transfer*, 34 (1991), 1, pp. 253-266
- [2] Kudo, K., *et al.*, Analysis on Inverse Radiative Property Problem in Two-Dimensional Systems, *ASME HTD*, 340 (1997), 2, pp. 135-140
- [3] Siewert, C. E., Inverse Solutions to Radiative-Transfer Problems with Partially Transparent Boundaries and Diffuse Reflection, *J. Quantitative Spectroscopy Radiative Transfer*, 72 (2002), 4, pp. 299-313
- [4] Milandri, A., Asllanaj, F., Jeandel, G., Determination of Radiative Properties of Fibrous Media by an Inverse Method-Comparison with the Mie Theory, *J. Quantitative Spectroscopy Radiative Transfer*, 74 (2002), 5, pp. 637-653

- [5] Kim, K. W., et al., Estimation of Emissivities in a Two-Dimensional Irregular Geometry by Inverse Radiation Analysis Using Hybrid Genetic Algorithm, *J. Quantitative Spectroscopy Radiative Transfer*, 87 (2004), 1, pp.1-14
- [6] Kim, K. W., Baek, S. W., Efficient Inverse Radiation Analysis in a Cylindrical Geometry Using a Combined Method of Hybrid Genetic Algorithm and Finite-Difference Newton Method, *J. Quantitative Spectroscopy Radiative Transfer*, 108 (2007), 3, pp. 423-439
- [7] Qi, H., et al., Inverse Radiation Analysis of a One-Dimensional Participating Slab by Stochastic Particle Swarm Optimizer Algorithm, *Int. J. Thermal Sciences*, 46 (2008), 7, pp. 649-661
- [8] McCormick, N. J., Inverse Radiative Transfer Problems: A Review, *Nucl. Sci. Eng.*, 112 (1992), 3, pp. 185-198
- [9] Grissa, H., et al., Three-Dimensional Radiative Transfer Modeling Using the Control Volume Finite Element Method, *J. Quantitative Spectroscopy Radiative Transfer*, 105 (2007), 3, pp. 388-404
- [10] Grissa, H., et al., Nonaxisymmetric Radiative Transfer in Inhomogeneous Cylindrical Media with Anisotropic Scattering, *J. Quantitative Spectroscopy Radiative Transfer*, 109 (2008), 3, pp. 494-513
- [11] Grissa, H., et al., Prediction of Radiative Heat Transfer in 3D Complex Geometries Using the Unstructured Control Volume Finite Element Method, *J. Quantitative Spectroscopy Radiative Transfer*, 111 (2010), 2, pp. 144-154
- [12] Lazard, M., et al., Radiative and Conductive Heat Transfer: A Coupled Model for Parameter Estimation, *High Temperatures-High Pressures*, 32 (2000), 1, pp. 9-17
- [13] Kim, K. W., Baek, S. W., Inverse Radiation-Conduction Design Problem in a Participating Concentric Cylindrical Medium, *Int. J. Heat Mass Transfer*, 50 (2007), 13, pp. 2828-2837
- [14] Zhao, S. W., Zhang, B. M., Du, S. Y., An Inverse Analysis to Determine Conductive and Radiative Properties of a Fibrous Medium, *J. Quantitative Spectroscopy Radiative Transfer*, 110 (2009), 13, pp. 1111-1123
- [15] Marquardt, D. W., An algorithm for Least Squares Estimation of Nonlinear Parameters, *J. Social Industrial Applied Mathematics*, 11 (1963), 2, pp.431-441
- [16] Fiveland, W. A., Three Dimensional Radiative Heat Transfer Solutions by Discrete Ordinates Method, *J. Thermophysics Heat Transfer*, 2 (1988), 4, pp. 309-316
- [17] Coelho, P. J., A Hybrid Finite Volume/Finite Element Discretization Method for the Solution of the Radiative Heat Transfer Equation, *J. Quantitative Spectroscopy Radiative Transfer*, 93 (2005), 1, pp. 89-101